Soft Matter

RSC Publishing

PAPER

Gelation of the genome by topoisomerase II targeting anticancer agents†

Cite this: *Soft Matter*, 2013, **9**, 1656

Yun Soo Kim,‡[a] Binu Kundukad,‡[a] Abdollah Allahverdi,[b] Lars Nordensköld,[b] Patrick S. Doyle*[ac] and Johan R. C. van der Maarel*[ad]

Received 27th September 2012
Accepted 20th November 2012

DOI: 10.1039/c2sm27229f

www.rsc.org/softmatter

Topoisomerase II (TOP2) regulates the topology of DNA by catalysis of a double strand passage reaction. Inhibition of this reaction prevents cell replication, and, thus, is a pathway targeted by anticancer drugs. Some details regarding the cell-killing mechanism are unknown and assays to screen for anticancer drugs are not well established. Here, we study the gelation of linear and circular DNA using microrheology assays. Gelation of the DNA–enzyme mixture was examined by tracking of multiple colloidal probe particles. The mean square displacements of the probe particles were analyzed by the time-cure superposition procedure as well as the classical derivation of the dynamic moduli. First, the passage reaction was inhibited by AMP-PNP, a non-hydrolyzable analog of ATP. The results showed gelation due to the formation of a self-catenated network of circular DNA molecules. Next, when TOP2 was inhibited by the anti-cancer drug ICRF-193, we observed a similar change in rheology. Based on these findings, we propose a cell-killing mechanism by gelation of the genome through TOP2-mediated interlocking of looped DNA segments of the replicated, intertwined chromosomes.

1 Introduction

Topoisomerase II (TOP2) regulates chain entanglement in processes such as replication, transcription, and repair. Driven by the hydrolysis of ATP, the enzyme captures two strands of DNA and transposes their positions *via* a cleavage mediated double strand passage reaction.[1] Interlocking of DNA rings by TOP2 in the presence of polyvalent cations resulted in a self-catenated network, but no large structures were formed after inhibition with novobiocin or nalidixic acid.[2,3] TOP2 is a target for cancer therapeutics, because it is involved in chromatid motion and chromosome condensation in late stages of cell division.[4] TOP2 targeting drugs can be divided into two categories: the poisons and inhibitors.[5] The poisons stabilize DNA cleavage complexes and thus cause TOP2 to become a cytotoxic agent. The inhibitors block the passage reaction, but they are believed not to damage DNA. Some important details regarding the mechanism of the latter category are not clear. In particular, the relative importance of catalytic inhibition and/or the formation of a network need further investigation. Here, we report gelation resulting from interlocking of circular DNA molecules (catenation), mediated by the inhibition of TOP2.

We have investigated adenylyl-imidodiphosphate (AMP-PNP) and *meso*-4,4′-(3,2-butanediyl)-bis(2,6-piperazine-dione) (ICRF-193 or ICRF). AMP-PNP is a β,γ-imido analog of ATP and a model inhibitor of TOP2. It binds to TOP2 in the same way as ATP, but it cannot be hydrolyzed. Triggered by the binding of AMP-PNP, TOP2 closes, cannot be re-opened, and is converted to an annular form.[6,7] A double-strand passage reaction occurs, if a second segment has been captured before closure. The reaction rate of this one and only catalytic cycle is about a factor of 20 slower than the one in the presence of ATP.[8] Passage of two segments pertaining to two different circular DNA molecules results in catenation. Accordingly, for a dense solution of rings, we expect the formation of a network of interlocked DNA molecules. ICRF is a member of the bisdioxopiperazine class of anticancer agents. It binds to the interface of the dimerized ATP-ase domains of TOP2 and prevents reopening of the entrance N-gate. Note that ICRF does not compete for the ATP binding site, as is the case for AMP-PNP. ATP is required for closure, but ATP is not needed to maintain the closed state. Binding of ICRF results in a protein clamp around DNA, as for AMP-PNP.[9,10] As in the case of AMP-PNP, inhibition of TOP2 by ICRF is expected to result in a self-catenated network of circular DNA molecules. The extent to which such a network is formed as well as the role of DNA topology (linear *versus* circular) will be gauged with our microrheology assays.

[a]*BioSystems and Micromechanics, Singapore-MIT Alliance for Research and Technology, Singapore*

[b]*Nanyang Technological University, School of Biological Sciences, Singapore 63755*

[c]*Department of Chemical Engineering, Massachusetts Institute of Technology, Cambridge, Massachusetts 02139, USA. E-mail: pdoyle@mit.edu*

[d]*Department of Physics, National University of Singapore, Singapore 117542. E-mail: johanmaarel@gmail.com*

† Electronic supplementary information (ESI) available. See DOI: 10.1039/c2sm27229f

‡ These authors contributed equally to this work.

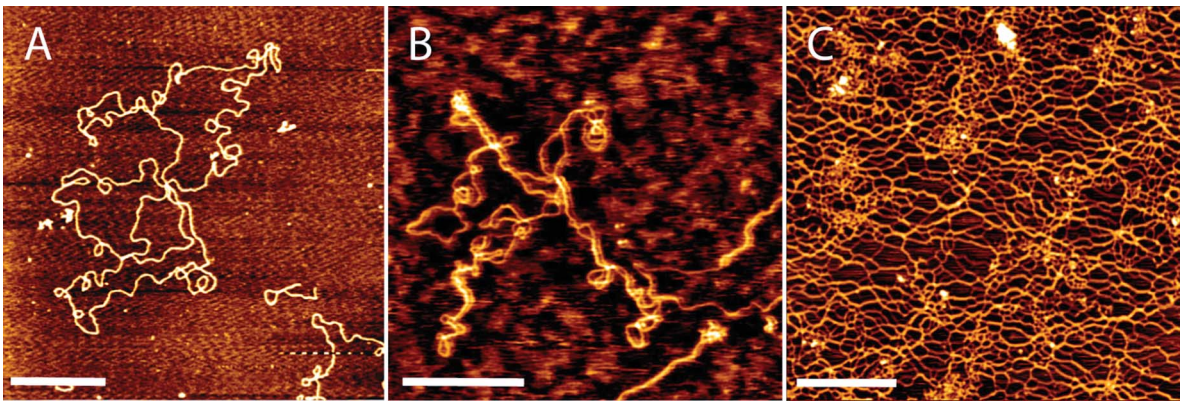

Fig. 1 Atomic force microscopy images of open circular (A), branched supercoiled (B), and gelated (C) cosmid. The gel is catenated with 4 units of TOP2 per μg of DNA and 2.5 mM AMP-PNP. The scale bars denote 500 nm.

We have used linear λ-DNA (48.5 kbp) and a circular cosmid. The cosmid is the Lawrist-4 vector with a 40 kbp insert from the human chromosome 1q21 (total size of 45 kbp).[11,12] Gel electrophoresis shows that about 95% of the cosmid is circular (see below). Our DNAs are hence of comparable molecular weight, but they differ in topology. Atomic force microscopy images of the cosmid are shown in Fig. 1. The enzyme is human topoisomerase IIα. DNA, enzyme, and inhibitor are dispersed in buffer and assayed with microrheology at 310 K (at ambient temperature there is no effect on the rheology). We have used video tracking of the Brownian motion of colloidal beads, which requires minute samples of no more than 15 μL each.[14,15] The amount of energy stored elastically (elastic storage modulus, G') and that lost through flow (viscous loss modulus, G''), as being the real and imaginary parts of the complex stress to strain ratio, are then obtained from the one-sided Fourier transform of the mean square displacement $\langle \Delta x^2 \rangle$ of the beads.[18] First, the rheology of the cosmid assay has been investigated at the relevant temperature and buffer composition. These experiments serve as a reference and were done without TOP2. Second, we have explored the effect of TOP2 in conjunction with ATP and AMP-PNP. Third, we have studied the effect of ICRF. Comparison of the results obtained for ATP, the two inhibitors, and the two DNAs will then provide information about gelation.

2 Materials and methods

2.1 Chemicals, enzymes, and DNAs

Human topoisomerase IIα (TOP2) was purchased from Affymetrix. As supplied by the manufacturer, the TOP2 storage buffer contains 15 mM Na_2HPO_4, pH 7.1, 700 mM NaCl, 0.1 mM EDTA, 0.5 mM dithiothreitol (DTT), and 50% glycerol. The reaction buffer is composed of 10 mM Tris–HCl, pH 7.9, 50 mM NaCl, 50 mM KCl, 5 mM $MgCl_2$, 0.1 mM EDTA, and 15 mg L^{-1} bovine serum albumin. Adenosine-triphosphate (ATP), adenylyl-imido-diphosphate (AMP-PNP), and *meso*-4,4′-(3,2-butanediyl)-bis(2,6-piperazinedione) (ICRF-193) were purchased from Sigma-Aldrich. Water was deionized and purified by a Millipore system and has a conductivity less than 1×10^{-6} Ω^{-1} cm^{-1}. λ-DNA was purchased from New England Biolabs, Ipswich, MA. A 12 base long oligonucleotide with the complementary sequence of the right cohesive end of λ-DNA, 5′-AGGTCGCCGCCC-3′, was purchased from Sigma-Aldrich. The solution was concentrated to a concentration of 1.8 g of DNA per L by freeze drying and subsequently dialyzed in microdialyzers against TOP2 reaction buffer. The DNA concentration was determined by UV spectrometry. The stock solution was heated to 333 K, cooled to 295 K by immersion in a water bath, and the complimentary oligonucleotide was hybridized to one of the overhangs with a 100% excess molar ratio.

The cosmid, with a total size of 45 kbp, is derived from the Lawrist-4 vector and contains a 40 kbp insert from the human chromosome 1q21.[11,12] A colony of *Escherichia coli* DH5α was transformed on a LB agar plate with kanamycin (50 mg L^{-1}). A single colony was taken to grow a culture in terrific broth (TB) medium (12 g of tryptone, 24 g of yeast extract, 4 mL of glycerol, 12.5 g of K_2HPO_4 and 2.3 g of KH_2PO_4 per L) and kanamycin (50 mg L^{-1}) at 310 K. After 6 h, this culture was put into flasks, which contained a total of 7.5 L TB medium and kanamycin. The bacteria were cultured for 19 h at 310 K under continuous shaking and, subsequently, harvested. The cells were suspended in TEG buffer (20 mM Tris, 10 mM EDTA, 50 mM glucose, pH 8.0) and lysed with an alkaline solution (1% SDS, 0.2 M NaOH). Bacterial genomic DNA, cellular debris, and proteins were precipitated by the addition of 4 M potassium acetate and 2 M acetic acid followed by incubation on ice. RNA and protein were removed with an RNAse (20 mg L^{-1}, 310 K, 12 h) treatment and phenol extraction, respectively. After precipitation with ethanol, the pellet was dried for a short time, suspended in TE buffer (10 mM Tris–HCl, 0.1 mM EDTA, pH 8.5) and, eventually dialyzed against the reaction buffer with a final concentration of 3.5 g of cosmid per L.

2.2 Gel electrophoresis

The integrity of the cosmid and λ-DNA was checked with pulsed field inversion 1% agarose gel electrophoresis in TAE buffer (40 mM Tris-acetate, 1 mM EDTA, pH 8.3) at 6 V cm^{-1} for 9 h. The gel image obtained by ethidium bromide staining is shown in Fig. 2. In order to assign the different bands in the

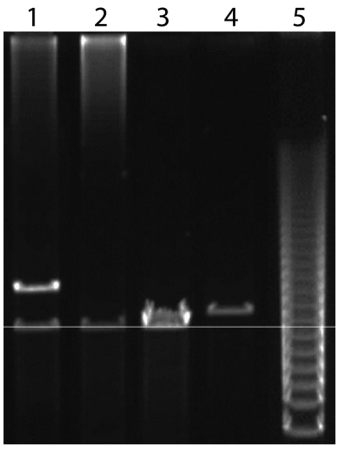

Fig. 2 Pulsed gel electrophoresis. The lanes are: (1) cosmid; (2) cosmid after treatment with TOP2; (3) linearized cosmid after treatment with NruI; (4) λ-DNA; (5) ladder. The line demarcates the migration distance for 45 kbp linear DNA.

chromatogram, we have treated the cosmid with TOP2 and restriction endonuclease NruI (New England Biolabs). After treatment with TOP2, the closed circular, supercoiled cosmid is relaxed with linking number deficits $\Delta Lk = 0$ or ± 1. The circular cosmid is converted into a linear form by the endonuclease. The chromatogram of the cosmid preparation shows a weak band at 45 kbp and an intense band at a slightly lower migration distance of around 55 kbp. After treatment with TOP2, the intense band at around 55 kbp disappears. Concurrently, a smear next to the loading reservoir appears and there is no appreciable change in intensity of the weak band at 45 kbp. The linearized cosmid shows no smear and a single broad band around 45 kbp. From these results we conclude that the strong and weak bands at 55 and 45 kbp correspond to the cosmid in the tightly interwound supercoiled and linear form, respectively. The smear comes from open circular DNA, branched supercoils, as well as DNAs with low degree of supercoiling. From the integrated band intensities we conclude that 5% of the cosmid is in the linear form. Furthermore, neither degradation nor multimerization of hybridized λ-DNA was observed.

2.3 Atomic force microscopy

Solution droplets (0.5 mg cosmid per L of reaction buffer) were spotted on freshly cleaved mica, incubated for 15 min, rinsed with deionized water, nitrogen gas-dried, and imaged at room temperature in air with a Nanowizard 2 atomic force microscope (JPK Instruments, Berlin, Germany). The gel could not be diluted with buffer, nor washed away with water, and was imaged directly after spotting 20 μL on mica. Images were acquired in the tapping mode with silicon (Si) cantilevers (spring constant of 10–130 N m^{-1}) and operated below their resonance frequency (typically 204–497 kHz). The contrast and brightness were adjusted for optimum viewing conditions.

2.4 Sample preparation

Samples were prepared by dilution of the stock solution with reaction buffer. After dilution, but before the addition of the enzyme, all samples were equilibrated at least overnight. Three series of experiments were done. For the first series, solutions with concentrations of 0.7, 1.7, and 2.4 g of cosmid per L were prepared. These solutions do not contain TOP2 and provide the blanks. In the second series, we investigated the effect of AMP-PNP in conjunction with TOP2 on the properties of the flow. For this purpose, TOP2 was added to solutions of 1.6 g of cosmid per L in ratios of 2, 4, and 6 units per μg of DNA with an AMP-PNP concentration of 2.5 mM. We also prepared a solution of 1.6 g of cosmid per L with 4 units of TOP2 per μg of DNA and an ATP concentration of 2.5 mM. In the third series, TOP2 inhibition with ICRF-193 is investigated. Here, TOP2 was added to solutions of 1.6 g of cosmid per L in ratios of 2 and 6 (1 mM ICRF-193 only) units per μg with an ATP concentration of 2.5 mM and ICRF-193 concentrations of 0.1 and 1 mM, respectively. We have also investigated solutions of 1.0 g of λ-DNA per L with 4 units per μg of TOP2. The latter solutions also contained 2.5 mM AMP-PNP or 2.5 mM ATP and 1 mM ICRF-193. One unit of TOP2 (20 ng) is the amount of enzyme required to fully relax 0.3 μg of negatively supercoiled pBR322 plasmid DNA in 15 min at 303 K under standard assay conditions. With a molecular weight of 340 kDa, one unit per μg of cosmid DNA (45 kbp) corresponds with 1.7 dimers per DNA molecule. All samples were spiked with polystyrene fluorescence microspheres (Bangs Laboratories, IN) of 1.9 ± 0.2 μm diameter with a final concentration of 0.08 wt%. The microspheres are internally labeled with dragon green with a maximal excitation and emission wavelength of 480 and 520 nm, respectively. Just before the microrheology experiment, we added about 2 μL of the enzyme in storage buffer to 10 μL of DNA in reaction buffer, followed by mixing the solution for 20 s through gentle stirring and pipetting up and down. Shear was minimized by using pipette tips that have wide openings. A droplet of solution was deposited on a microscopy slide and sealed with a coverslip separated by a 0.2 mm spacer. The slide is subsequently loaded on the pre-heated and temperature controlled stage of the microscope. All measurements were done at 310 K. All samples were assayed at least in duplicate. The initial time is taken as the time when the specimen was loaded on the preheated microscopy stage.

2.5 Microrheology

Particle tracking experiments were done at 310 K with an inverted Olympus IX71 fluorescence microscope equipped with a 50× long working distance objective, numerical aperture of 0.35, and an ALPHA Vivid XF100-3 filter set (Omega Optics, Brattleboro, VT). In order to minimize hydrodynamic interactions, the imaged beads are separated by at least 10 bead diameters (20 μm). Furthermore, the focal plane was adjusted to be midway between the glass slide and coverslip. Video was collected with an electron multiplying charge coupled device (EMCCD) camera (Andor iXon 897) and Andor Solis software. We have checked our setup by measuring the diffusion of colloidal beads dispersed in a concentrated solution of glycerol as well as by monitoring immobilized beads adsorbed at a glass slide. The tracking experiment was started within 1 min after

addition of the enzyme. A series of video clips was recorded with a rate of 107 frames per second, full frame size of 128 × 128 pixels, and exposure time of 1 ms. The exposure time is short enough to minimize dynamic error and the static error in $\langle \Delta x^2 \rangle$, as estimated by monitoring immobilized beads, is around 10 nm.[13] Each clip has a duration of 100 s and the total duration of the movie is 100 min. The clips were taken randomly in the *xy* plane and in each clip the trajectories of 2 to 6 particles were recorded. Accordingly, 120 to 360 different particles constitute each ensemble averaged mean square displacement, but the maximum lag time is 100 s due to the finite duration of the clips. The video was analyzed with MATLAB (Natick, MA) and the particle trajectories were obtained with public domain tracking software (http://physics.georgetown.edu/matlab/). All further data analysis was done with home-developed software scripts written in MATLAB code.[14,15] The pixel size in the *x*- and *y*-directions of 0.32 μm was determined with a metric ruler.

3 Results and discussion

3.1 Viscoelasticity without enzyme

We have first explored the viscoelasticity of our model system at the relevant temperature and buffer composition, but without enzyme. For this purpose, we have measured $\langle \Delta x^2(t) \rangle$ of the beads for a series of samples with increasing concentration of cosmid. The results are displayed in Fig. 3A. The cosmid concentrations are well above the overlap concentration of around 0.1 g of cosmid per L, as estimated from the radius of gyration and the overlap concentration for linear DNA.[16,17] Diffusive behavior with $\langle \Delta x^2 \rangle \propto t$ is only observed for very long times and/or low DNA concentrations. With increasing concentration of DNA, $\langle \Delta x^2 \rangle$ decreases and the range of times with a subdiffusive scaling exponent less than one becomes wider. This behavior is typical for a viscoelastic fluid and is more conveniently discussed in terms of G' and G''.[18]

Following the procedure as described before,[15] we have obtained the moduli from the one-sided Fourier transform of $\langle \Delta x^2(t) \rangle$ and the generalized Stokes–Einstein equation. The moduli are displayed in Fig. 3B. An important observation is that all samples show viscous fluidlike behavior with $G' < G''$ and G'' approaching $\propto \omega$ at low frequencies. The moduli increase with increasing frequency. For a concentration exceeding, say 1.5 g of cosmid per L, G' becomes larger than G'' above a certain cross-over frequency. This behavior is qualitatively similar to what has previously been observed for λ-DNA.[14,15] Quantitatively, there are differences in the values of the moduli (at least an order of magnitude less for the cosmid) and the critical concentration for the development of viscoelasticity (0.5 g L^{-1} for λ-DNA). These differences agree with the reported higher viscosity and lower diffusivity of linear *versus* circular DNA.[19,20] However, a discussion of the effect of topology on the viscoelasticity is beyond the scope of the present contribution. Here, we focus on the effect of TOP2 in conjunction with TOP2 targeting anticancer agents on the viscoelasticity.

3.2 Inhibition with AMP-PNP

Time series microrheology experiments were done with TOP2 and AMP-PNP. For this purpose, we added 2, 4, or 6 units of TOP2 per μg of DNA to solutions of 1.6 g of cosmid per L. One unit per μg of cosmid corresponds with 1.7 protein dimers per molecule. The AMP-PNP concentration is 2.5 mM. Note that these solutions do not contain ATP, so the protein dimers are immediately converted into clamps during their first and only catalytic cycle. For reference, we have also investigated a solution of 1.6 g of cosmid per L with 4 units of TOP2 per μg of DNA and 2.5 mM ATP. The trajectories of the beads were binned into time intervals of various durations. We observed that the time scale of the change in $\langle \Delta x^2 \rangle$ (min) is much longer than the one pertaining to the loss of correlation in the velocity of the beads (s). Within each interval, the system is in quasi-equilibrium with Gaussian distributions in the displacements of the beads. Accordingly, for each interval $\langle \Delta x^2 \rangle$ and, subsequently, G' and G'' were obtained as described before.[15] The time evolution of G' and G'' after the addition of 2, 4, and 6 units of TOP2 per μg of

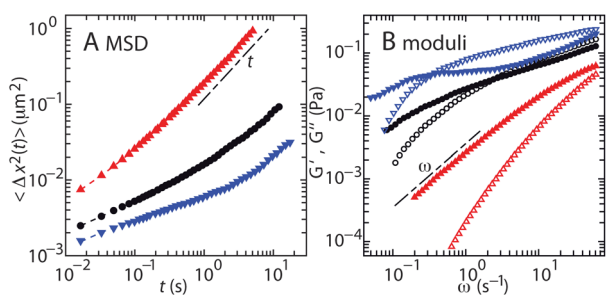

Fig. 3 (A) Mean square displacement $\langle \Delta x^2 \rangle$ *versus* time *t* in reaction buffer at 310 K. The concentrations are 2.4 (blue, downward triangles), 1.7 (black, circles), and 0.7 (red, upward triangles) g of cosmid per L. (B) Storage G' (open symbols) and loss G'' (closed symbols) moduli *versus* frequency ω. The dashed-dotted lines denote the scaling laws for the diffusive $\langle \Delta x^2 \rangle \propto t$ and low shear $G'' \propto \omega$ limits for long times and low frequencies, respectively.

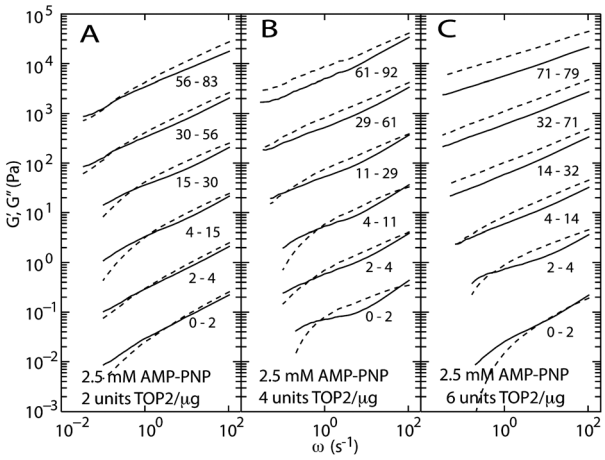

Fig. 4 (A) Time evolution of G' (dashed curves) and G'' (solid curves) after the addition of TOP2 to a solution of 1.6 g of cosmid per L with 2.5 mM AMP-PNP (ATP-free). The TOP2 concentration is 2 units per μg of DNA. (B) As in panel (A), but with 4 units of TOP2 per μg. (C) As in panel (A), but with 6 units of TOP2 per μg. Time intervals are indicated in min. The moduli are shifted with a multiplicative factor 10 along the *y*-axis to avoid overlap.

cosmid with 2.5 mM AMP-PNP is shown in Fig. 4. The result for the reference sample with 4 units of TOP2 per μg of cosmid and 2.5 mM ATP is shown in Fig. 5. The corresponding (shifted) mean square displacements are shown in Fig. 6 and the ESI,† respectively.

Initially, the solutions containing AMP-PNP show viscous fluidlike behavior at low frequencies ($G' < G''$ and $G'' \propto \omega$). With increasing reaction time, the cross-over frequency shifts to lower values. Eventually, with 4 and 6 units TOP2 per μg of DNA, elastic behavior is observed with parallel scaling of the moduli and $G' > G''$ for all frequencies (Fig. 4). In the case of 2 units per μg, the solution becomes more viscoelastic, but no gelation was observed within the time span of our experiment (80 min). As shown in Fig. 5, with ATP rather than AMP-PNP, there is no qualitative change in moduli. As shown by gel electrophoresis in Fig. 2, the cosmid is relaxed by TOP2 and ATP.[21] The moderate relative increase in G' with respect to G'' is hence likely due to unwinding and concomitant increase in size of the supercoil. In the presence of ATP, viscous fluidlike behavior is observed for all reaction times (Fig. 5). A comparison of G' and G'' obtained with AMP-PNP and ATP, respectively, shows that TOP2 needs to be inhibited in order for DNA to form a gel. Gelation due to cross-links made of protein or protein aggregates can be excluded, because no significant change in moduli was observed following digestion of TOP2 by proteinase K. An atomic force microscopy image of the gel is shown in Fig. 1C.

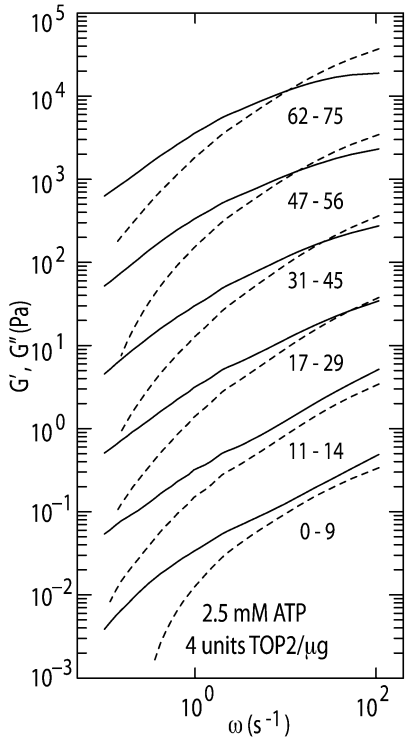

Fig. 5 Time evolution of G' (dashed curves) and G'' (solid curves) after the addition of TOP2 to a solution of 1.6 g of cosmid per L with 2.5 mM ATP (AMP-PNP-free). The TOP2 concentration is 4 units per μg of DNA. Time intervals are indicated in min. The moduli are shifted with a multiplicative factor 10 along the *y*-axis to avoid overlap.

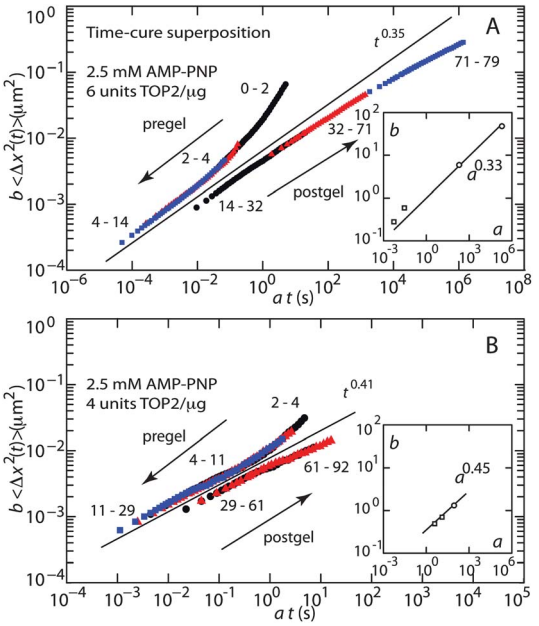

Fig. 6 (A) Pre- and postgel master curves obtained by superposing $\langle \Delta x^2 \rangle$ for 1.6 g of cosmid per L, 2.5 mM AMP-PNP, and 6 units of TOP2 per μg of DNA. The pre- and postgel curves are arbitrarily shifted to avoid overlap. Time intervals are indicated in min. (Inset) Power law scaling of shift factor *b versus* shift factor *a* (squares, pregel; circles, postgel). (B) As in panel (A), but with 4 units of TOP2 per μg.

The gelation time has been estimated with the time-cure superposition formalism.[22,23] Two master curves, pre- and postgel, are formed by multiplication of t with a and $\langle \Delta x^2 \rangle$ with b. Shift factors a and b were chosen to yield the best superposition of $\langle \Delta x^2 \rangle$ in terms of gradient and curvature. The result pertaining to 6 and 4 units of TOP2 per μg of cosmid and 2.5 mM AMP-PNP is shown in Fig. 6. At the gel point, the shape of the master curve changes from convex to concave and $\langle \Delta x^2 \rangle \propto t^n$, with critical exponent n. With 4 and 6 units of TOP2 per μg of DNA, the gelation times are around 30 and 15 min, respectively. The corresponding values of n are 0.41 ± 0.02 and 0.35 ± 0.02, indicating a more elastic critical gel for higher TOP2 concentration. Note that the values for n are consistent with critical scalings of the shift factors at the gel point ($b \propto a^n$, see insets of Fig. 6).

The equilibrium behavior of the moduli is shown in Fig. 7. The corresponding mean square displacements are shown in the ESI.† Here, the reaction time exceeds 1 h and no appreciable change in moduli was observed for longer times. We have included the results for λ-DNA obtained with 4 units of TOP2 per μg of DNA and 2.5 mM AMP-PNP. The effect of (non)-inhibited TOP2 on the viscoelasticity of λ-DNA was reported before.[14] For λ-DNA and in the presence of AMP-PNP, there is only a temporary increase in G' after the addition of the enzyme. For longer times, exceeding, say, 20 min, there is no qualitative change in the moduli. In the case of linear DNA there is no transition to a gel as observed for the cosmid. Note that λ-DNA and the cosmid are of comparable molecular weight, they only differ in topology. These results confirm that for linear DNA no network is formed.

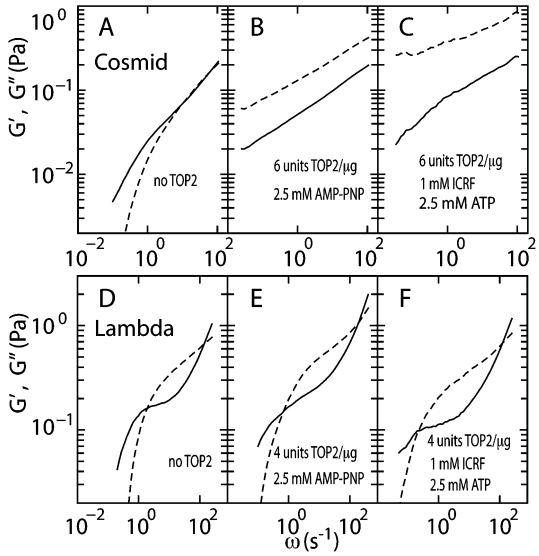

Fig. 7 (A–C) G' (dashed curves) and G'' (solid curves) for a solution of 1.6 g of cosmid per L. (A) No added TOP2; (B) 6 units of TOP2 per μg and 2.5 mM AMP-PNP; (C) 6 units of TOP2 per μg, 2.5 mM ATP, and 1 mM ICRF. (D–F) As in panels (A–C), but for 1.0 g of λ-DNA per L. (D) No added TOP2; (E) 4 units of TOP2 per μg and 2.5 mM AMP-PNP; (F) 4 units of TOP2 per μg, 2.5 mM ATP, and 1 mM ICRF. The samples are incubated at 310 K for 1 h after addition of TOP2.

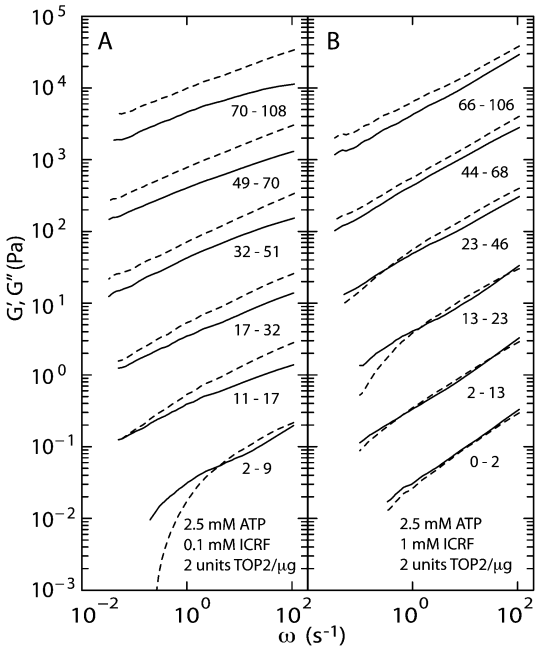

Fig. 8 (A) Time evolution of G' (dashed curves) and G'' (solid curves) after the addition of TOP2 to a solution of 1.6 g of cosmid per L. The TOP2 concentration is 2 units per μg, the ATP concentration is 2.5 mM, and the ICRF-193 concentration is 0.1 mM. (B) As in panel (A), but with an ICRF-193 concentration of 1 mM. The time intervals are in min and the moduli are shifted with a factor 10 along the *y*-axis.

The number of catenates, *i.e.*, interlocks formed by catenation, per molecule can be gauged from the high frequency behavior of the elasticity modulus. In general, the elasticity modulus is given by the density of dynamic units times thermal energy k_BT.[24] In the absence of catenates, the dynamic units are the individual DNA molecules. The elasticity modulus G is then given by the Rouse modulus $G_R = \rho k_BT$, with DNA density ρ (provided the molecules are not entangled). In the interlocked network, the dynamic units are strands between the catenates. Let N_c be the number of catenates per molecule, so that the density of the strands between the catenates is given by $N_c\rho$. The elasticity modulus hence reads $G = N_cG_R$ and N_c can be obtained from the ratio of the post- and pregel elasticity modulus G/G_R. We can unfortunately not determine the high frequency limits of the elasticity modulus due to the absence of a plateau value within our finite window of observation. Nevertheless, comparison of the high frequency behavior of G' in Fig. 7A and B indicates that only about two catenates per molecule are formed with 6 units of TOP2 per μg of cosmid and 2.5 mM AMP-PNP. The molecules are hence weakly interconnected.

3.3 Inhibition with ICRF-193

Next, we have inhibited TOP2 with ICRF. For this purpose, 2 or 6 units of TOP2 per μg of DNA were added to solutions of 1.6 g of cosmid per L. The solutions also contained 0.1 or 1 mM ICRF and 2.5 mM ATP. ATP is needed for initial closure of the enzyme, but not to maintain the closed state.[9] With increasing reaction time, TOP2 is progressively converted into clamps by binding of ICRF.[10] The time evolution of G' and G'' after the addition of 2 units of TOP2 per μg of DNA in the presence of 0.1 and 1 mM ICRF is displayed in Fig. 8. The shifted mean square displacements are shown in Fig. 9. For a cosmid solution with 6 units of TOP2 per μg of DNA, 2.5 mM ATP, and 1 mM

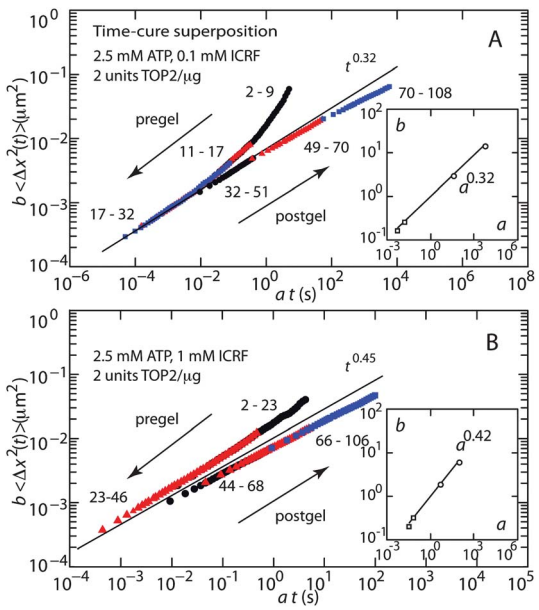

Fig. 9 (A) Pre- and postgel master curves obtained by superposing $\langle\Delta x^2\rangle$ for 1.6 g of cosmid per L, 2.5 mM ATP, 0.1 mM ICRF, and 2 units of TOP2 per μg of DNA. The pre- and postgel curves are arbitrarily shifted to avoid overlap. Time intervals are indicated in min. (Inset) Power law scaling of shift factor *b versus* shift factor *a* (squares, pregel; circles, postgel). (B) As in panel (A), but with 1 mM ICRF.

Table 1 Summary of gelation times and critical exponents under various experimental conditions

Inhibitor, TOP2 units per μg	Gel time (min)	Critical exponent n
2.5 mM AMP-PNP, 6	15	0.35 ± 0.02
2.5 mM AMP-PNP, 4	30	0.41 ± 0.02
0.1 mM ICRF,[a] 2	30	0.32 ± 0.02
1 mM ICRF,[a] 2	45	0.45 ± 0.02

[a] Solutions also contained 2.5 mM ATP.

ICRF, the equilibrium moduli are displayed in Fig. 7. The corresponding moduli of a solution of λ-DNA with 4 units of TOP2 per μg of DNA, 2.5 mM ATP, and 1 mM ICRF are also shown in Fig. 7. As in the case of AMP-PNP, there is no appreciable change in moduli of linear DNA following inhibition of TOP2 by ICRF.

Pre- and postgel master curves pertaining to 2 units of TOP2 per μg of DNA with 0.1 and 1 mM ICRF are shown in Fig. 9. The gelation time and stiffness of the gel depends on the initial concentrations of ICRF and TOP2. For instance, in the case of 2 units of TOP2 per μg of DNA, the gelation times are around 30 and 45 min with 0.1 and 1 mM ICRF, respectively. Furthermore, with a concentration of 1 mM ICRF a weaker critical gel is observed with $n = 0.45 \pm 0.02$ compared to the one obtained with 0.1 mM ICRF ($n = 0.32 \pm 0.02$). This observation indicates that catenation is more efficient at low concentrations of ICRF. At high concentrations of ICRF, inhibition is fast due to rapid binding of ICRF. However, more TOP2 is wasted by closures without capture of a second DNA segment, resulting in a clamp on DNA, but no passage reaction and, hence, no catenation. With 6 units of TOP2 per μg of DNA, 2.5 mM ATP, and 1 mM ICRF, the gelation time becomes very short (a few min) and the final gel becomes stronger than the one observed with AMP-PNP (see Fig. 7B and C). Comparison of the high frequency behavior of G' in Fig. 7A and C indicates that about 5 catenates per molecule are formed with 6 units of TOP2 per μg of cosmid and 1 mM ICRF. Since there are 10 protein dimers per molecule, this implies that 50% of the inhibited enzyme results in catenation. The gelation times and critical exponents are collected in Table 1. Quantitative comparison shows that the DNA–enzyme mixtures with the model inhibitor AMP-PNP and the anti-cancer agent ICRF exhibit similar properties of gelation.

4 Conclusions

Our observations can be summarized as follows. Qualitatively similar results are obtained with AMP-PNP and ICRF. In the case of circular DNA, gelation is observed. For linear DNA, there is no appreciable change in viscoelasticity for longer reaction times. With increasing TOP2 concentration, the gelation time becomes shorter and the final gel becomes stronger. More efficient gelation is observed in the case of a lower concentration of ICRF. Without an inhibitor, but in the presence of ATP, no gelation was observed. All of these results agree with the formation of a network of interlocked DNA molecules. A prerequisite is that the DNA molecule or segment thereof is circular or looped, because double-strand passage of a linear molecule does not result in a network. The gelation time is the time required for long-range connectivity and depends on TOP2 concentration and inhibition efficiency. In the presence of ATP, the continuous activity of the enzyme prevents the formation of a network by *de*catenation of interlocked molecules.

At least 3 cell-killing mechanisms by bisdioxopiperazines have been proposed.[5] It is widely believed that ICRF is a pure catalytic inhibitor. It has also been suggested that ICRF stabilizes strand passing intermediates and thus causes TOP2 to become a DNA damaging agent.[25] In the third proposed mechanism the closed clamp conformation trapped on DNA interferes with DNA metabolic processes, resulting in cell death.[26] Late stages of chromosome condensation and segregation are blocked by ICRF.[4] It is our contention that this is caused by gelation through TOP2-mediated interlocking of looped DNA segments of the intertwined replicated chromosomes. Besides this new insight into the killing mechanism, the microrheology assay provides a convenient screening technology for the relevant class of topoisomerase targeting cancer therapeutics.

Acknowledgements

This work is supported by the Singapore-MIT Alliance for Research and Technology and National Science Foundation grant [CBET-0852235] and the Singapore Ministry of Education grant [R-144-000-256-112]. Claude Backendorf is thanked for the gift of the cosmid.

References

1 J. C. Wang, *Q. Rev. Biophys.*, 1998, **31**, 107–144.
2 M. A. Krasnow and N. Cozzarelli, *J. Biol. Chem.*, 1982, **257**, 2687–2693.
3 W. Waldeck, M. Theobald and H. Zentgraf, *EMBO J.*, 1983, **2**, 1255–1261.
4 R. Ishida, M. Sato, T. Narita, K. R. Utsumi, T. Nishimoto, T. Morita, H. Nagata and T. Andoh, *J. Cell Biol.*, 1994, **126**, 1341–1351.
5 J. L. Nitiss, *Nat. Rev. Cancer*, 2009, **9**, 338–350.
6 J. Roca and J. C. Wang, *Cell*, 1992, **71**, 833–840.
7 J. Roca and J. C. Wang, *Cell*, 1994, **77**, 609–616.
8 C. L. Baird, T. T. Harkins, S. K. Morris and J. E. Lindsley, *Proc. Natl. Acad. Sci. U. S. A.*, 1999, **96**, 13685–13690.
9 J. Roca, R. Ishida, J. M. Berger, T. Andoh and J. C. Wang, *Proc. Natl. Acad. Sci. U. S. A.*, 1994, **91**, 1781–1785.
10 S. Classen, S. Olland and J. M. Berger, *Proc. Natl. Acad. Sci. U. S. A.*, 2003, **100**, 10629–10634.
11 S. H. Cross and P. F. R. Little, *Gene*, 1986, **49**, 9–22.
12 A. Cabral, P. Voskamp, A. M. Cleton-Jansen, A. South, D. Nizetic and C. Backendorf, *J. Biol. Chem.*, 2001, **276**, 19231–19237.
13 T. Savin and P. S. Doyle, *Biophys. J.*, 2005, **88**, 623–638.
14 B. Kundukad and J. R. C. van der Maarel, *Biophys. J.*, 2010, **99**, 1906–1915.
15 X. Zhu, B. Kundukad and J. R. C. van der Maarel, *J. Chem. Phys.*, 2008, **129**, 185103.

16 R. M. Robertson, S. Laib and D. E. Smith, *Proc. Natl. Acad. Sci. U. S. A.*, 2006, **103**, 7310–7314.
17 R. Verma, J. C. Crocker, T. C. Lubensky and A. G. Yodh, *Phys. Rev. Lett.*, 1998, **81**, 4004–4007.
18 T. G. Mason, *Rheol. Acta*, 2000, **39**, 371–378.
19 A. Goodman, Y. Tseng and D. Wirtz, *J. Mol. Biol.*, 2002, **323**, 199–215.
20 R. M. Robertson and D. E. Smith, *Proc. Natl. Acad. Sci. U. S. A.*, 2007, **104**, 4824–4827.
21 A. D. Bates and A. Maxwell, *DNA Topology*, Oxford University Press, Oxford, 1993.
22 T. H. Larsen and E. M. Furst, *Phys. Rev. Lett.*, 2008, **100**, 146001.
23 A. M. Corrigan and A. M. Donald, *Langmuir*, 2009, **25**, 8599–8605.
24 P.-G. de Gennes, *Scaling Concepts in Polymer Physics*, Cornell University Press, Ithaca, NY, 1979.
25 K. C. Huang, H. Gao, E. F. Yamasaki, D. R. Grabowski, S. Liu, L. L. Shen, K. K. Chan, R. Ganapathi and R. M. Snapka, *J. Biol. Chem.*, 2001, **276**, 44488–44494.
26 L. H. Jensen, K. C. Nitiss, A. Rose, J. Dong, J. Zhou, T. Hu, N. Osheroff, P. B. Jensen, M. Sehested and J. L. Nitiss, *J. Biol. Chem.*, 2000, **275**, 2137–2146.